

Hemicellulose-Based Multifunctional Macroinitiator for Single-Electron-Transfer Mediated Living Radical Polymerization

Jens Voepel,[†] Ulrica Edlund,[†] Ann-Christine Albertsson,^{*,†} and Virgil Percec[‡]

Fibre- and Polymer Technology, Royal Institute of Technology (KTH), SE-100 44 Stockholm, Sweden, and Roy and Diana Vagelos Laboratories, Department of Chemistry, University of Pennsylvania, Philadelphia, Pennsylvania 19104-6323, United States

Received November 15, 2010; Revised Manuscript Received December 3, 2010

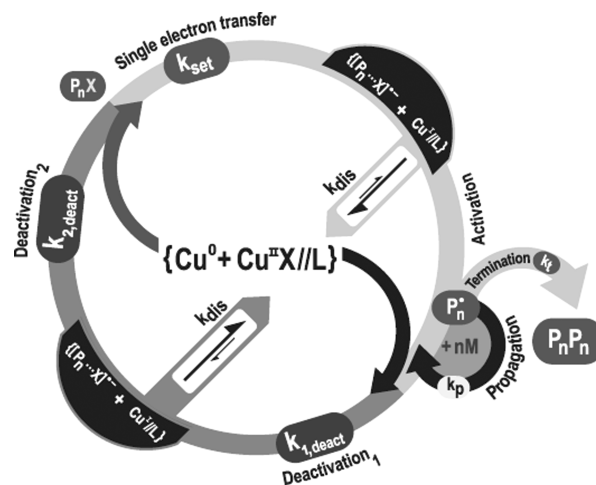
A multifunctional macroinitiator for single-electron-transfer mediated living radical polymerization (SET-LRP) was designed from acetylated galactoglucomannan (AcGGM) by α -bromoisobutyric acid functionalization of the anomeric hydroxyl groups on the heteropolysaccharide backbone. This macroinitiator, with a degree of substitution of 0.15, was used in the SET-LRP of methyl acrylate, catalyzed by Cu⁰/Me₆-TREN in DMSO, DMF, or DMSO/H₂O in various concentrations. Kinetic analyses confirm high conversions of up to 99.98% and a living behavior of the SET-LRP process providing high molecular weight hemicelluloses/methyl acrylate hybrid copolymers with a brush-like architecture.

Introduction

Single-electron-transfer mediated living radical polymerization (SET-LRP) has emerged as a potent method to achieve living radical polymerization,^{1–3} and the concept is currently being elaborated and explored with respect to mechanism,^{4–12} reaction conditions,^{13–19} polymer topology, and architecture,^{20–22} as well as suitable monomers.^{23–25} The metal-catalyzed synthetic pathway involves the reversible activation of a halide-terminated macroradical [P_n-X] into an active propagating chain P_n•. The metal catalyst is typically a Cu species, such as Cu⁰, Cu₂O, or Cu₂S, which donates a single electron to the halide-terminated chain, causing a heterolytic cleavage of the carbon-halide bond via the formation of a radical anion that dissociates into P_n• and X⁻ and enables propagation.^{1,2} The Cu^I species generated in the SET process associate with an N-ligand to form a Cu^IX/L complex. Fast disproportionation of this complex leads to the formation of a Cu⁰ and a Cu^{II}X₂/L. The latter mediates the deactivation of the propagating macroradical generating the dormant species [P_n-X]. The proposed SET-LRP cycle is schematically outlined in Scheme 1.

Although recently introduced, SET-LRP has already been proved a facile and versatile strategy for living radical polymerization.² SET-LRP is viable for a range of monomers, including the commercially important acrylates,^{22,26,27} acrylamides,^{28,29} vinyl chloride,^{1,23,30} styrene,³¹ methacrylates,^{24,32–35} and methacrylic acid.³⁶ A number of different ligands and initiators have also been shown eligible for SET-LRP. The most efficient initiators for SET-LRP and for Atom Transfer Radical Polymerization (ATRP) must match the reactivity of the propagating dormant chain. The most efficient solvents (dipolar aprotic, alcohols, water and combinations of them) and ligands (Me₆-TREN) for SET-LRP are those that form stronger complexes with Cu(II)X₂ rather than Cu(I)X species and therefore, mediate the disproportionation of Cu(I)X into Cu(0) and Cu(II)X₂. Both differ from the nonpolar solvents and ligands

Scheme 1. Catalytic Cycle of SET-LRP Based on Cu⁰ in Polar Solvents



required for ATRP that form stronger complexes with Cu(I)X species. Compared to ATRP, which involves the Cu(I)X activating species, the SET-LRP is more robust in the sense that the activation rate constant of propagation is not strongly determined by the nature of the halide (X = Cl, Br, or I).¹¹ In addition, SET-LRP can be successfully conducted without a vigorous deoxygenation process by the addition of an extremely small amount of reducing agent to the reaction mixture, allowing for an economical approach to the synthesis of functional macromolecules.¹³ This is considered a major advantage of SET-LRP over ATRP, since the AGET (activator generated by electron transfer) and ARGET (activator regenerated by electron transfer) ATRP conducted under limited air require the addition of excess reducing agent as oxygen scavenger.^{37,38} The high tolerance to O₂ of SET-LRP was further exemplified by its “immortal” nature.¹² Despite repeated interruptions by O₂, the reactivated SET-LRP provides polymers with narrow molecular weight distribution and excellent chain-end functionality.¹² The addition of O₂ to ATRP would irreversibly oxidize the active Cu(I)X species and terminate the polymerization process.

* To whom correspondence should be addressed. E-mail: aila@kth.se.

[†] Royal Institute of Technology (KTH).

[‡] University of Pennsylvania.

It was recently shown that markedly increased reaction rates, suppression of induction periods, and better control of the polymer chain ends can be achieved in SET-LRP via a reducing pretreatment of the catalyst surface to ensure high Cu^0 availability rather than a combination of Cu_2O and $\text{Cu}(0)$ that is available on the surface of nonreduced $\text{Cu}(0)$ catalyst.¹⁸

The versatility and controllability of the SET-LRP strategy opens up a range of possibilities to use this method for the site-specific controlled grafting from functionalized sites on macromolecules thereby producing graft copolymers and brush-like structure.^{22,29,32} As such, the method is appealing for the design of hybrid materials from macromolecules that do not otherwise lend themselves to vinyl copolymerization, such as polymers based on sugar moieties, known as polysaccharides. An abundant, inexpensive, renewable, and green candidate from this family is acetylated galactoglucomannan, a softwood hemicellulose. We have previously demonstrated its viability and versatility as a candidate for various chemical modifications and the development of functional materials.^{39–47}

Several attempts have been presented for the vinyl copolymerization with polysaccharides into glycopolymers, including the controlled free radical polymerization with sugar derivatives,²³ covalent linkage of PMMA chains to cellulose,⁴⁸ styrene grafting on cellulose filter paper⁴⁹ via reversible addition–fragmentation chain transfer (RAFT), or the grafting onto chitosan.⁵⁰ However, these reactions have several drawbacks, such as high reaction temperatures, water sensibility, low conversions, and a risk for cross-linking.

Here, SET-LRP offers a unique opportunity of targeted functionalization of the aforementioned acetylated galactoglucomannan. Being soluble in dimethyl sulfoxide (DMSO), *N,N*-dimethylformamide (DMF) and H_2O this polysaccharide offers the chance to graft polymer chains from the backbone in a one phase system. Thus, this method offers a new approach, achieving brush-like architectures with equally long polymer chains randomly distributed on the AcGGM backbone derived in homogeneous media in contrast to earlier reports being heterogeneous grafting from surfaces.

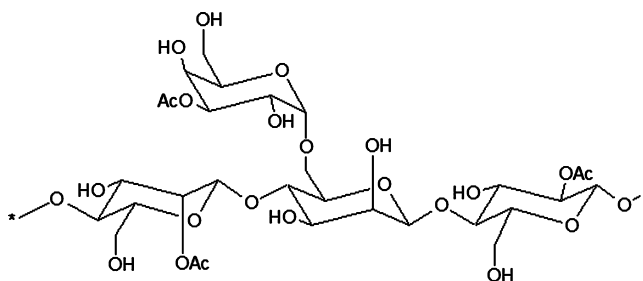
Experimental Section

Materials. *N,N'*-Carbonyldiimidazole (CDI) 97% (Aldrich), α -bromoisobutyric acid (α BrIBA) 98% (Aldrich), tris(2-aminoethyl)amine 96% (Aldrich), formic acid $\geq 96\%$ (Aldrich), formaldehyde_{aq} 37% (Alfa Aesar), dichloromethane 99.8% (Fisher), sodium chloride 99.5% (Merck), 2-propanol $\geq 99\%$ (LabScan), methanol $\geq 99.8\%$ (Labscan), copper wire (Gauge 20) (Fisher), acetone (Fischer, purum), and dimethylacetamide 99.8% (Fisher) were used as received. Dimethyl sulfoxide (DMSO) $\geq 99.5\%$ (Fluka), *N,N*-dimethylformamide (DMF) 99.8% (Fisher), and methyl acrylate (MA) 99.0% (Merck) were distilled at reduced pressure prior to use.

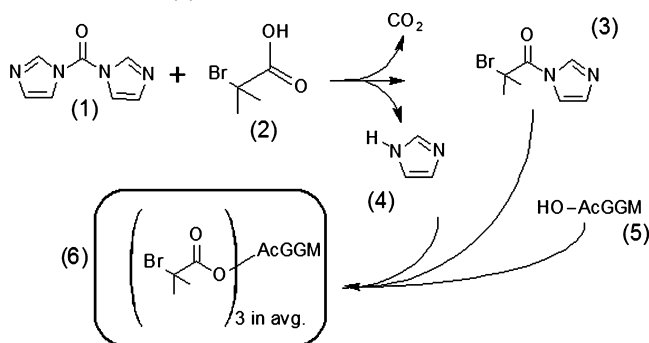
O-Acetyl-galactoglucomannan (AcGGM) originating from spruce (*Picea abies*) was extracted from thermomechanical pulping process water, fractionated by ultrafiltration and finally freeze-dried. The sugar composition was 17% glucose, 65% mannose, 15% galactose.⁵¹ The average molecular weight was about 7500 g mol^{-1} (DP ~ 40), the PDI was ~ 1.3 , and the degree of acetylation (DS_{Ac}) was 0.30, as determined by size exclusion chromatography (SEC) calibrated with MALDI-TOF-MS. A representative structure of AcGGM is shown in Scheme 2.

Esterification of AcGGM. The AcGGM macro initiator was synthesized performing a *N,N'*-carbonyldiimidazole (CDI)-assisted esterification of the hydroxyl groups of the polysaccharide backbone as depicted in Scheme 3. In a first step, 9.73 g CDI (60 mmol, 4 equiv) was reacted with 10.02 g α -bromoisobutyric acid (α BrIBA; 60 mmol, 4 equiv) in 80 mL of DMSO at room temperature for 60 min to form

Scheme 2. Representative Structural Unit of Acetylated Galactoglucomannan



Scheme 3. CDI (1) Assisted Coupling of α -bromoisobutyric Acid (2) under CO_2 Expulsion to 3-bromo-1-(1*H*-imidazol-1-yl)-3-methylbutan-1-one (3), Followed by Imidazole (4)-Catalyzed Esterification of Acetylated Galactoglucomannan (5) to α -BriBA-AcGGM (6)

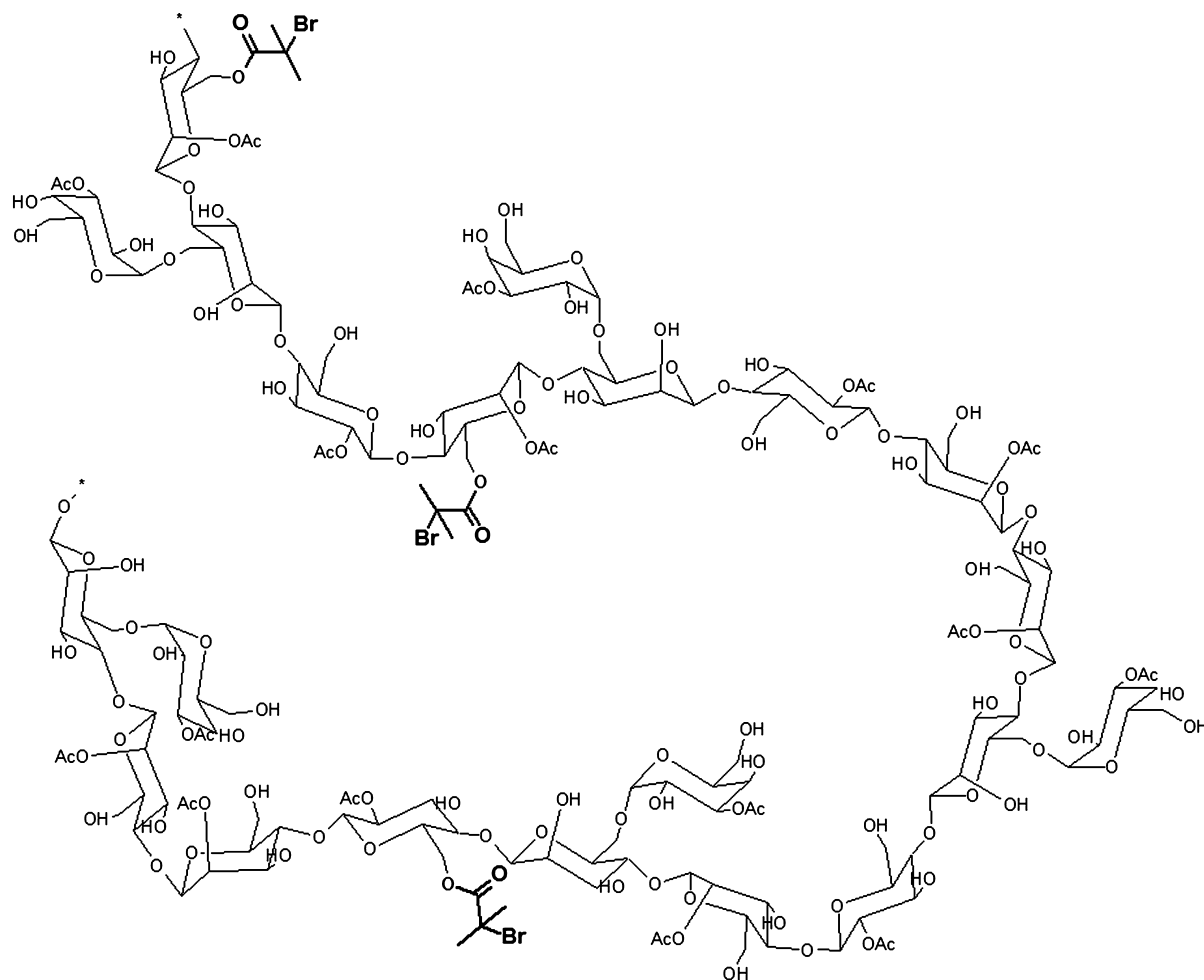
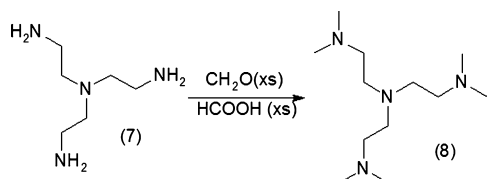
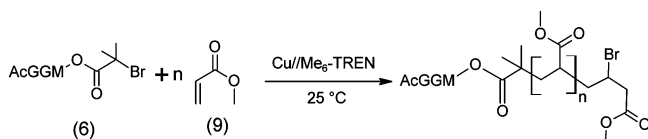


the imidazolyl-activated acid derivative. Following, 4.08 g imidazole (60 mmol, 4 equiv) were added as additional catalyst and the reaction mixture was heated to 50°C . To this solution 2.60 g AcGGM (15 mmol hexose units, 1 equiv) in 100 mL of DMSO were added under stirring at 50°C . The reaction was stopped after 60 to 120 min, was precipitated in 2-propanol, followed by centrifugal collection and Soxhlet extraction for 2 days with 2-propanol.

The macroinitiator is representatively shown in Scheme 4, including half of the main chain repeating units with respect to the degree of polymerization estimated by SEC. An average macroinitiator molecule is expected to consist of approximately 40 sugar rings with three –Br initiator moieties.

$\text{Me}_6\text{-TREN}$ Synthesis. $\text{Me}_6\text{-TREN}$ was synthesized as reported earlier.⁵² A total of 25.5 mL of 98% formic acid (0.45 mol, 10 equiv) and 25 mL of 37% formaldehyde (0.30 mol, 6.65 equiv) were mixed in a round-bottom flask kept in an ice bath. Tris(2-aminoethyl)amine (6.58 g, 0.045 mol, 1 equiv) in 25 mL of H_2O were added dropwise to the solution, keeping the reaction mixture at 0°C . After 60 min, the ice bath was removed and the solution was allowed to warm up to room temperature. Then the flask was heated to 100°C and refluxed overnight. After removing the volatiles at reduced pressure in a rotary evaporator, the orange residue was adjusted to pH 10 with NaOH_{aq} (10% w/w). The crude product was extracted with dichloromethane, the organic phase repeatedly washed with H_2O and NaCl solution and the product was recovered via rotary evaporation at reduced pressure. Low pressure distillation yielded an oily, colorless liquid. The synthesis of $\text{Me}_6\text{-TREN}$ is shown in Scheme 5. ^1H NMR ($\text{DMSO}-d_6$): δ 2.50 ppm (tr, 6 H, CH_2), 2.26 (tr, 6 H, CH_2), 2.12 (s, 18 H, $\text{N}-\text{CH}_3$); ^{13}C NMR ($\text{DMSO}-d_6$): δ 57.43, 52.52, 45.64 ppm.

Polymerizations. Polymerizations were conducted in DMSO, $\text{DMSO}/\text{H}_2\text{O}$, or DMF. Ligand ($\text{Me}_6\text{-TREN}$), macroinitiator (Br-AcGGM), and monomer (methyl acrylate, MA) in a 1:10:2000 as well as a 1:10:4000 molar ratio were dissolved in DMSO or DMF. Typical amounts were 1.4 μL of $\text{Me}_6\text{-TREN}$ (0.005 mmol), 50.95 mg Br-AcGGM (0.05 mmol -Br), and 860 mg MA (10 mmol) in 3 mL of solvent. As catalyst, 6.25 or 12.5 cm of copper wire (20 gauge) was wrapped around the stirring bar for all polymerizations. The solution was transferred to a Schlenk-

Scheme 4. Representative Structure of the Functionalized Macroinitiator Based on AcGGM**Scheme 5.** Me₆-TREN (8) is Synthesized via an Eschweiler–Clarke Methylation, Reacting Tris(2-aminoethyl)amine (7) with Formaldehyde and Formic Acid in Excess**Scheme 6.** SET-LRP of MA (9) with α -BriBA-AcGGM (6) as Macroinitiator

tube and degassed with six freeze–pump–thaw cycles, flushing with nitrogen after thawing. Next, the tube was transferred to an oil bath at 25 °C and the stirring bar was dropped into the solution, starting the polymerization. The proceeding polymerization, as schematically illustrated in Scheme 6, was monitored via ¹H NMR (for conversion) and SEC (for molecular weight), taking samples with a steel syringe at various times under constant nitrogen flow. Products were precipitated in methanol and dried prior to SEC-measurements.

Characterization. The molecular weights were determined from filtered samples by Size Exclusion Chromatography (SEC) on a system based on *N,N*-dimethylacetamide as eluent, with a flow rate of 0.5 mL/min at 80 °C. Pullulan standards with narrow molecular weight distributions were used for calibration.

¹H and ¹³C NMR spectra were recorded at 500 MHz on a Bruker DMX-500 nuclear magnetic resonance spectrometer using Bruker software. Samples of about 20 mg were dissolved in DMSO-*d*₆ or D₂O (Larodan Fine Chemicals AB) in 5 mm o.d. sample tubes.

Thermograms were recorded by Differential Scanning Calorimetry (DSC) using a temperature- and energy-calibrated Mettler Toledo DSC 820 purged with nitrogen gas (80 mL/min). The samples were loaded into 100 μ L aluminum caps. Thermograms were recorded from –30 to 200 °C at a heating rate of 10 °C/min by a heating–cooling–heating cycle. Glass transition temperatures were determined from the second heating.

Results and Discussion

A macroinitiator based on the heteropolysaccharide acetylated galactoglucomannan (AcGGM) was designed to enable the use of SET-LRP as a new and powerful approach for the synthesis of hybrid glycopolymers under benign conditions. The synthetic route includes (1) esterification of the polysaccharide affording bromine groups in α position linked to the backbone, (2) the Cu⁰-catalyzed, living radical polymerization of a representative vinyl monomer yielding graft copolymers with a brush-like architecture. Reaction kinetics and molecular weights of the resulting hybrid materials are herein elaborated.

Esterification of AcGGM. The CDI-assisted esterification was preferred to acid halides due to observed degradation of the polysaccharide during the esterification experiments performed with the acid halide. The AcGGM-macroinitiator was synthesized via the imidazolyl-activated α -bromoisobutyric acid

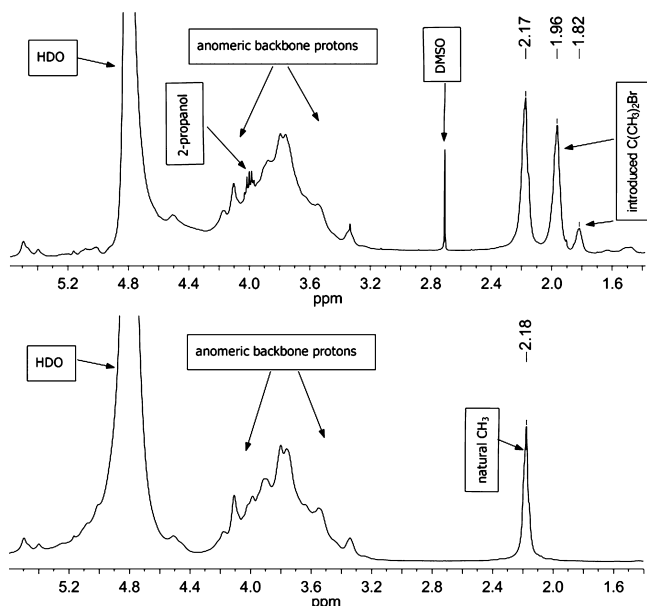


Figure 1. ^1H NMR spectra of the natural AcGGM (bottom) and of the macroinitiator (top).

(α -BrIBA) under CO_2 and imidazole elimination in the first step. The byproduct imidazole catalyzes the covalent coupling to the AcGGM backbone via esterification.

The precipitated and thoroughly washed product was analyzed by ^1H NMR, as shown in Figure 1. Here, the methyl groups of the coupled species shift dependent on their position on the polysaccharide backbone at 1.96 and 1.82 ppm. Knowing that the natural degree of acetylation is 0.3, the incorporated methyl groups and thus the amount of coupled initiator can be quantified in relation to the signal of the acetyl group at 2.17 ppm. Residual traces of 2-propanol (around 4 ppm) and DMSO (at 2.71 ppm) are visible but do not affect the quantitative evaluation of the product.

Because the probability of having propagating sites situated in the vicinity of another propagating macroradical in its active state is increasing with the degree of substitution (DS), a moderate DS was chosen. Thus, all polymerizations in this work were conducted with a macroinitiator DS of 0.15, corresponding to one α -bromine per 6.6 hexose units in average. SEC analysis revealed a moderate degradation to ~ 7000 g/mol.

Me₆-TREN Synthesis. Me₆-TREN was synthesized by performing an Eschweiler–Clark reaction. Tris(2-aminoethyl)-amine was 6-fold methylated, reacting it with excess formic acid and formaldehyde under CO_2 and H_2O elimination. Extraction and purification resulted in a rather low final yield (13%) but high purity, as proven with ^1H and ^{13}C NMR. ^1H NMR (DMSO- d_6): δ 2.50 (tr, 6 H, CH_2), 2.26 (tr, 6 H, CH_2), 2.12 (s, 18 H, N-(CH_3)₂); ^{13}C NMR (DMSO- d_6): δ 57.43, 52.52, 45.64 ppm.

Polymerizations. Polymerizations were first conducted in DMSO with a ligand/macroradical/MA molar ratio of 1/10/2000. Here, the macroinitiator concentration was constrained by the limited solubility in the reaction mixture with increasing monomer concentrations. As shown in Figure 2, the maximum initiator concentration of 16.6 mmol/L resulted in a living process with the apparent rate constant of propagation (k_p^{app}) of 0.0075 min^{-1} up to 90% conversion. However, due to the multifunctionality of the macroinitiator, at high conversion, multiple propagating macroradicals can terminate by recombination and cause gelation when originating from different macroinitiators. Accordingly, gel formation was observed at conversions of 60% and higher, growing adjacently to the copper wire and outward, swollen in the reaction media. Occurring cross-linking did slow down the process, resulting in a decrease of k_p^{app} to 0.0038 min^{-1} due to lowered mobility of the active centers as well as hindered monomer diffusion. Still, the reaction proceeded to almost full conversion, producing an insoluble fraction. However, due to the gel formation, taken samples may not be representative, which might explain the outliers in Figure 2. The molecular weight (M_n) of the soluble fraction increases linearly with reaction time and approaches 65000 g/mol at full conversion.

Hence, further experiments were designed to achieve slower reaction rates via lowering the radical concentration $[\text{P}^\bullet]$, thereby suppressing gelation as an undesired side reaction. As discussed earlier, reaction rates in SET-LRP can be enhanced by a reductive pretreatment of the Cu wire to increase the catalyst surface Cu^0 availability and due to a larger amount of $\text{Cu}(\text{II})\text{X}_2$ generated by disproportionation with a substantial improvement of the living polymerization process.¹⁸ Here, we focused on reducing the rate of polymerization by decreasing the catalyst concentration to avoid gelation.

To overcome the observed gel formation at high macro initiator concentration, reaction conditions were adapted by decreasing the initiator concentration to 4.16 mmol/L as well as reducing monomer and ligand concentration by 50% and, in addition, the Cu wire to 6.25 cm. However, this did not result in a decrease of k_p^{app} being 0.0043 min^{-1} here as well. Importantly, no gelation occurred even at full conversion (Figure 3).

Following, a polymerization with a higher initiator/monomer ratio was conducted. Here, a further decrease of the initiator concentration to 2.08 mmol/L was necessary to avoid too high viscosity, making sampling impossible at higher conversions. As seen in Figure 4, this resulted in a significantly decreased k_p^{app} of 0.0016 min^{-1} . Nevertheless, the reaction proceeded living until complete conversion. Increased viscosity and thus a nonrepresentative sampling at high conversion is seen as the reason for the outlier at 2880 min. Expected graft yield corresponds to around three PMA grafts per macroinitiator molecule which is reasonable

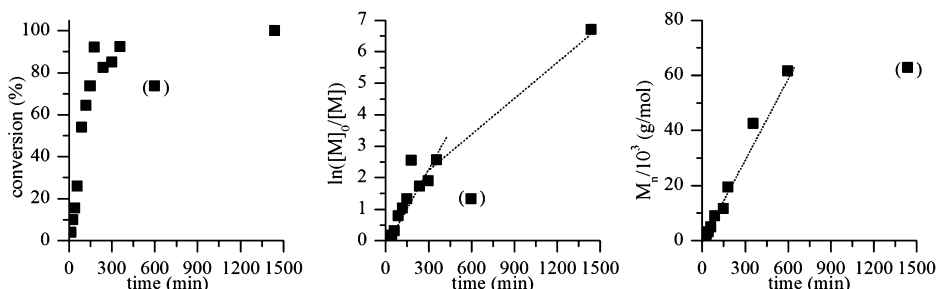


Figure 2. Kinetic plots for SET-LRP of MA ($L/I/M = 1/10/2000$), 12.5 cm Cu wire, and an initiator concentration of 16.6 mmol/L in DMSO.

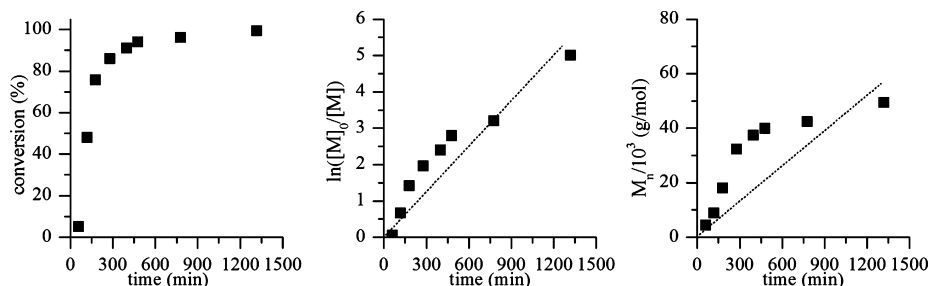


Figure 3. Kinetic plots for SET-LRP of MA ($L/I/M = 1/10/2000$), 6.25 cm Cu wire, and an initiator concentration of 4.16 mmol/L in DMSO.

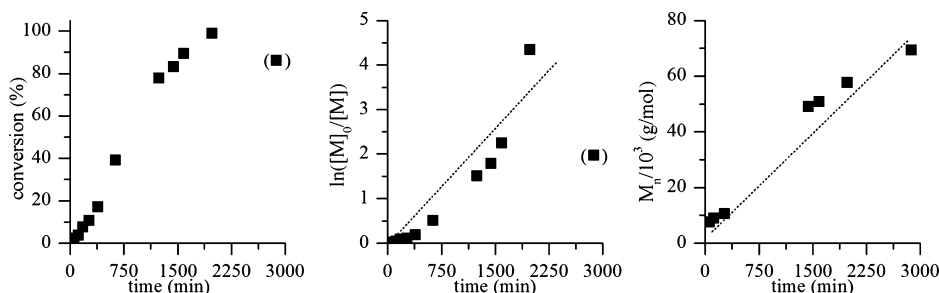


Figure 4. Kinetic plots for SET-LRP of MA ($L/I/M = 1/10/4000$), 6.25 cm Cu wire, and an initiator concentration of 2.08 mmol/L in DMSO.

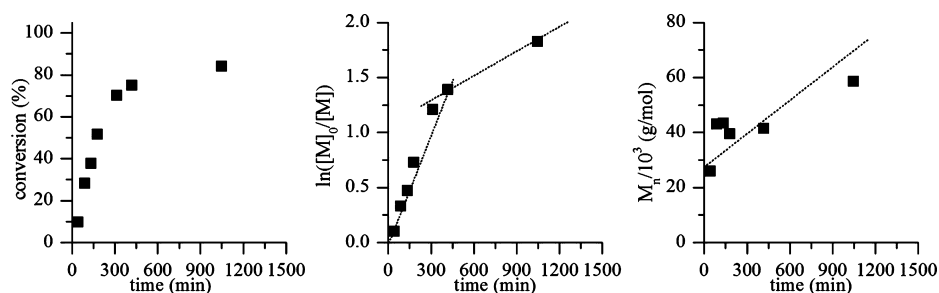


Figure 5. Kinetic plots for SET-LRP of MA ($L/I/M = 1/10/2000$), 6.25 cm Cu wire, and an initiator concentration of 4.16 mmol/L in a 90/10 (v/v) DMSO/H₂O solution.

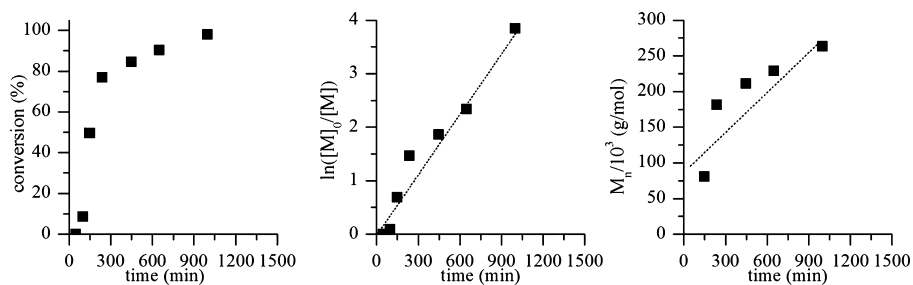


Figure 6. Kinetic plots for SET-LRP of MA ($L/I/M = 1/10/2000$), 6.25 cm Cu wire, and an initiator concentration of 4.16 mmol/L in DMF.

with respect to degree of substitution and steric effects. The molecular weights are here however less than expected. This is explained by the significant change in solubility parameters that affects the hydrodynamic volume and thus the calculated molecular weights.

Protic solvents like water are not only tolerated in SET-LRP but are actually shown to increase the rate of propagation due to the increased disproportionation of Cu(I)X into Cu(0) and Cu(II)X₂.^{2,16} Hence, a 90:10 (% v/v) DMSO/H₂O solution was evaluated for its applicability in the SET-LRP with an AcGGM-derived macroinitiator. Figure 5 shows the kinetic plots of this experiment. The reaction proceeds in a controlled way until precipitation at around 80% conversion. However,

k_p^{app} decreases from 0.0035 to 0.0007 min⁻¹ during the reaction as compared to 0.0043 min⁻¹ in pure DMSO. This can be attributed to a decreased solubility of the dormant chain end in the reaction mixture and, thus, a lowered concentration of active propagating macroradicals. The corresponding SET-LRP was conducted in DMF as well. Here, almost complete conversion was observed with a k_p^{app} of 0.0039 min⁻¹.

Polymerization in DMF (Figure 6) was observed to proceed with significantly lower viscosity as compared to DMSO. The molecular weight at full conversion is dramatically higher than expected based on the calculated graft yield. A contributing factor may be the tendency for agglomeration,

Table 1. Comparative Solubility Data

solvent	unmodified AcGGM	macroinitiator	PMA-grafted AcGGM at high conversion
H ₂ O	++ ^a	+ ^b	-- ^d
DMSO	++ ^a	++ ^a	++ ^a
DMF	+ ^b	+ ^b	++ ^a
DMAc	-- ^d	++ ^a	++ ^a
THF	-- ^d	-- ^d	- ^c
CHCl ₃	-- ^d	-- ^d	- ^c

^a ++, easily soluble. ^b +, slightly soluble. ^c -, agglomeration. ^d --, insoluble.

also observed during the synthesis and possibly preserved in liquid media resulting in a marked increase in hydrodynamic volume.

The poly(methyl acrylate), PMA, produced at high conversion by the described SET-LRP approach using an AcGGM-based macroinitiator have thermal properties similar to that of conventional PMA as compared to unmodified AcGGM that do not show any clear-cut glass transition. PMA derived by AcGGM-initiated SET-LRP with an initiator concentration of 4.16 mmol/L are amorphous with a glass transition temperature (T_g) between 15.7 and 19.7 °C. Commercial PMA is typically amorphous with a T_g around 6–9 °C.⁵³ The solubility properties for unmodified AcGGM, the AcGGM-derived macroinitiator, and PMA-grafted AcGGM at high conversion is summarized in Table 1.

Conclusions

The hemicellulose acetylated galactoglucomannan (AcGGM) was successfully functionalized by α -bromoisobutyric acid to a degree of substitution of 0.15 yielding a new and effective multifunctional macroinitiator for SET-LRP. SET-LRP of MA was performed at 25 °C catalyzed by Cu⁰/Me₆-TREN and the AcGGM-based macroinitiator yielding graft copolymers with molecular weights ranging from 4300 to 263,000 g mol⁻¹. The initiator concentration is limited by the tendency of product gelation. Kinetic analyses confirm the living character of the polymerizations and reveal a more rapid propagation in DMSO than in DMF or DMSO/H₂O (90:10% v/v) proceeding to almost full conversions regardless of the solvent used. AcGGM-initiated SET-LRP of MA is a powerful approach to the design of hybrid graft glycopolymers.

Acknowledgment. The authors gratefully acknowledge KTH and Formas (Project No. 243-2008-129) and for financial support.

References and Notes

- Percec, V.; Guliashvili, T.; Ladislav, J. S.; Wistrand, A.; Stjernedahl, A.; Sienkowska, M. J.; Monteiro, M. J.; Sahoo, S. *J. Am. Chem. Soc.* **2006**, *128* (43), 14156–14165.
- Rosen, B. M.; Percec, V. *Chem. Rev.* **2009**, *109* (11), 5069–5119.
- Matyjaszewski, K.; Tsarevsky, N. V.; Braunecker, W. A.; Dong, H.; Huang, J.; Jakubowski, W.; Kwak, Y.; Nicolay, R.; Tang, W.; Yoon, J. A. *Macromolecules* **2007**, *40* (22), 7795–7806.
- Lligadas, G.; Rosen, B. M.; Monteiro, M. J.; Percec, V. *Macromolecules* **2008**, *41* (22), 8360–8364.
- Lligadas, G.; Rosen, B. M.; Bell, C. A.; Monteiro, M. J.; Percec, V. *Macromolecules* **2008**, *41* (22), 8365–8371.
- Nguyen, N. H.; Rosen, B. M.; Lligadas, G.; Percec, V. *Macromolecules* **2009**, *42* (7), 2379–2386.
- Monteiro, M. J.; Guliashvili, T.; Percec, V. *J. Polym. Sci., Part A: Polym. Chem.* **2007**, *45* (10), 1835–1847.
- Rosen, B. M.; Percec, V. *J. Polym. Sci., Part A: Polym. Chem.* **2007**, *45* (21), 4950–4964.
- Rosen, B. M.; Percec, V. *J. Polym. Sci., Part A: Polym. Chem.* **2008**, *46* (16), 5663–5697.
- Jiang, X.; Fleischmann, S.; Nguyen, N. H.; Rosen, B. M.; Percec, V. *J. Polym. Sci., Part A: Polym. Chem.* **2009**, *47* (21), 5591–5605.
- Guliashvili, T.; Percec, V. *J. Polym. Sci., Part A: Polym. Chem.* **2007**, *45* (9), 1607–1618.
- Jiang, X. A.; Rosen, B. M.; Percec, V. *J. Polym. Sci., Part A: Polym. Chem.* **2010**, *48* (12), 2716–2721.
- Fleischmann, S.; Rosen, B. M.; Percec, V. *J. Polym. Sci., Part A: Polym. Chem.* **2010**, *48* (5), 1190–1196.
- Lligadas, G.; Percec, V. *J. Polym. Sci., Part A: Polym. Chem.* **2008**, *46* (20), 6880–6895.
- Nguyen, N. H.; Jiang, X.; Fleischmann, S.; Rosen, B. M.; Percec, V. *J. Polym. Sci., Part A: Polym. Chem.* **2009**, *47* (21), 5629–5638.
- Nguyen, N. H.; Rosen, B. M.; Jiang, X.; Fleischmann, S.; Percec, V. *J. Polym. Sci., Part A: Polym. Chem.* **2009**, *47* (21), 5577–5590.
- Rosen, B. M.; Jiang, X.; Wilson, C. J.; Nguyen, N. H.; Monteiro, M. J.; Percec, V. *J. Polym. Sci., Part A: Polym. Chem.* **2009**, *47* (21), 5606–5628.
- Nguyen, N. H.; Percec, V. *J. Polym. Sci., Part A: Polym. Chem.* **2010**, *48* (22), 5109–5119.
- Wright, P. M.; Mantovani, G.; Haddleton, D. M. *J. Polym. Sci., Part A: Polym. Chem.* **2008**, *46* (22), 7376–7385.
- Rosen, B. M.; Lligadas, G.; Hahn, C.; Percec, V. *J. Polym. Sci., Part A: Polym. Chem.* **2009**, *47* (15), 3940–3948.
- Lligadas, G.; Percec, V. *J. Polym. Sci., Part A: Polym. Chem.* **2007**, *45*, 4684–4695.
- Zhai, S.; Wang, B.; Feng, C.; Li, Y.; Yang, D.; Hu, J.; Lu, G.; Huang, X. *J. Polym. Sci., Part A: Polym. Chem.* **2010**, *48* (3), 647–655.
- Sienkowska, M. J.; Rosen, B. M.; Percec, V. *J. Polym. Sci., Part A: Polym. Chem.* **2009**, *47* (16), 4130–4140.
- Fleischmann, S.; Percec, V. *J. Polym. Sci., Part A: Polym. Chem.* **2010**, *48* (10), 2236–2242.
- Syrett, J. A.; Jones, M. W.; Haddleton, D. M. *Chem. Commun.* **2010**, *46* (38), 7181–7183.
- Tang, X.; Liang, X.; Yang, Q.; Fan, X.; Shen, Z.; Zhou, Q. *J. Polym. Sci., Part A: Polym. Chem.* **2009**, *47* (17), 4420–4427.
- Potisek, S. L.; Davis, D. A.; Sottos, N. R.; White, S. R.; Moore, J. S. *J. Am. Chem. Soc.* **2007**, *129*, 13808–13809.
- Nguyen, N. H.; Rosen, B. M.; Percec, V. *J. Polym. Sci., Part A: Polym. Chem.* **2010**, *48* (8), 1752–1763.
- Zoppe, J. O.; Habibi, Y.; Rojas, O. J.; Venditti, R. A.; Johansson, L.-S.; Efimenko, K.; Ölsterberg, M.; Laine, J. *Biomacromolecules* **2010**, *11* (10), 2683–2691.
- Hatano, T.; Rosen, B. M.; Percec, V. *J. Polym. Sci., Part A: Polym. Chem.* **2009**, *48* (1), 164–172.
- Tom, J.; Hornby, B.; West, A.; Harrison, S.; Perrier, S. *Polym. Chem.* **2010**, *1* (4), 420–422.
- Ding, S.; Floyd, J. A.; Walters, K. B. *J. Polym. Sci., Part A: Polym. Chem.* **2009**, *47* (23), 6552–6560.
- Fleischmann, S.; Percec, V. *J. Polym. Sci., Part A: Polym. Chem.* **2010**, *48* (10), 2251–2255.
- Fleischmann, S.; Percec, V. *J. Polym. Sci., Part A: Polym. Chem.* **2010**, *48* (10), 2243–2250.
- Fleischmann, S.; Percec, V. *J. Polym. Sci., Part A: Polym. Chem.* **2010**, *48* (21), 4889–4893.
- Fleischmann, S.; Percec, V. *J. Polym. Sci., Part A: Polym. Chem.* **2010**, *48* (21), 4884–4888.
- Matyjaszewski, K.; Dong, H.; Jakubowski, W.; Pietrasik, J.; Kusumo, A. *Langmuir* **2007**, *23* (8), 4528–4531.
- Min, K.; Jakubowski, W.; Matyjaszewski, K. *Macromol. Rapid Commun.* **2006**, *27* (8), 594–598.
- Hartman, J.; Albertsson, A. C.; Lindblad, M. S.; Sjöberg, J. *J. Appl. Polym. Sci.* **2006**, *100* (4), 2985–2991.
- Hartman, J.; Albertsson, A. C.; Sjöberg, J. *Biomacromolecules* **2006**, *7* (6), 1983–1989.
- Lindblad, M. S.; Sjöberg, J.; Albertsson, A. C.; Hartman, J. *ACS Symp. Ser.* **2007**, *954*, 153–167.
- Edlund, U.; Ryberg, Y. Z.; Albertsson, A. C. *Biomacromolecules* **2010**, *11* (9), 2532–2538.
- Roos, A. A.; Edlund, U.; Sjöberg, J.; Albertsson, A. C.; Stalbrand, H. *Biomacromolecules* **2008**, *9* (8), 2104–2110.
- Voepel, J.; Sjöberg, J.; Reif, M.; Albertsson, A. C.; Hultin, U. K.; Gasslander, U. *J. Appl. Polym. Sci.* **2009**, *112* (4), 2401–2412.
- Voepel, J.; Edlund, U.; Albertsson, A. C. *J. Polym. Sci., Part A: Polym. Chem.* **2009**, *47* (14), 3595–3606.
- Albertsson, A. C.; Voepel, J.; Edlund, U.; Dahlman, O.; Söderqvist-Lindblad, M. *Biomacromolecules* **2010**, *11* (5), 1406–1411.

- (47) Edlund, U.; Albertsson, A. C. *J. Bioact. Compat. Polym.* **2008**, *23* (2), 171–186.
- (48) Passirani, C.; Ferrarini, L.; Barratt, G.; Devissaguet, J. P.; Labarre, D. *J. Biomater. Sci., Polym. Ed.* **1999**, *10* (1), 47–62.
- (49) Roy, D.; Guthrie, J. T.; Perrier, S. *Macromolecules* **2005**, *38* (25), 10363–10372.
- (50) El Tahlawy, K.; Hudson, S. M. *J. Appl. Polym. Sci.* **2003**, *89* (4), 901–912.
- (51) Jacobs, A.; Lundqvist, J.; Stalbrand, H.; Tjerneld, F.; Dahlman, O. *Carbohydr. Res.* **2002**, *337* (8), 711–717.
- (52) Ciampolini, M.; Nardi, N. *Inorg. Chem.* **1966**, *5* (1), 41–44.
- (53) (a) Ulrich, H. *Introduction to Industrial Polymers*, 2nd ed.; Carl Hanser Verlag: Munich, Germany, 1993. (b) Sigma-Aldrich.

BM101357K